Modeling of Nonlinear Signal Distortion in Fiber-Optic Networks

Modeling of Nonlinear Signal Distortion in Fiber-Optic Networks

Pontus Johannisson and Erik Agrell

***Abstract*—A low-complexity model for signal quality prediction in a nonlinear fiber-optic network is developed. The model, which builds on the Gaussian noise model, takes into account the signal degradation caused by a combination of chromatic dispersion, nonlinear signal distortion, and amplifier noise. The center frequencies, bandwidths, and transmit powers can be chosen independently for each channel, which makes the model suitable for analysis and optimization of resource allocation and routing in large-scale optical networks applying flexible-grid wavelength-division multiplexing.**

***Index Terms*—Optical fiber communication, Optical fiber networks, Fiber nonlinear optics, Wavelength division multiplexing.**

I. Introduction

FIBER-OPTIC long-haul communication research has during the latest decade mainly been focused on coherent transmission. The data throughput has been increased by better utilization of the available bandwidth and receiver digital signal processing (DSP) has allowed many signal impairments to be compensated for. Further significant increase of the data rate is expected through the use of multicore/multimode fibers [1], but while this development is exciting, there are also significant challenges, e.g., the need for deployment of new fibers.

It is desirable to use available resources to the greatest possible extent and the increase in spectral efficiency enabled by coherent communication is a good example of this. For example, using a channel spacing of 50 GHz, it is now possible to transmit 100 Gb/s using polarization-multiplexed quadrature phase-shift keying. Comparing this with the traditional 10 Gb/s using on–off keying, the data throughput is increased by a factor of ten. In this work, the focus is on optical networking. By developing routing algorithms with awareness of the nonlinear physical properties of the channel, it would be possible to operate optical links closer to the optimum performance, and this would further increase the throughput in optical communication networks.

Optical networks are not as flexible as their electronic counterparts, but there are several efforts that aim at improving the situation by investigating, e.g., cognitive [2] and elastic [3] optical networks. An increased flexibility requires, e.g., hardware routing of channels in the optical domain and a monitoring system responsible for the resource allocation. It is also desirable that the coherent transmission and detection can be done using a number of different modulation formats and symbol rates, chosen dynamically in response to time-varying traffic demands and network load. Hence, the traditional wavelength-division multiplexing (WDM) paradigm, in which the available spectrum is divided into a fixed grid of equal-bandwidth channels, is being replaced by the concept of *flexible-grid* WDM [4].

A planning tool for allocation of resources such as routes, wavelengths, and bandwidth requires a model that quantifies the nonlinear signal distortion in the physical layer. While the problem of linear routing and wavelength assignment is well investigated, see, e.g., [5]–[8], the effort to find a nonlinear model that combines reasonable accuracy and low computational complexity is ongoing. Both these properties are necessary in order to be able to find a close-to-optimal solution and this excludes simulations of the nonlinear Schrödinger equation as an alternative. One approach is to build the performance estimation on a semi-analytical model and precalculate the necessary system parameters [9]. This allows accurate performance prediction and can take the correlation of nonlinear distortion generated in different fibers into account. However, such an approach relies on system-dependent numerical simulations and it is therefore desirable to complement this model with another one that has no free parameters and gives the performance estimate in an explicit way.

In this paper, we start from the Gaussian noise (GN) model [10]–[12] and derive a model that quantifies the nonlinear signal distortion in optical networks. The aim is to find a model that is useful both in real-time optimization, where demands for communication are added dynamically, and in offline mode, where a number of connections are to be optimized with respect to, e.g., bandwidth requirement or signal quality. It should be noticed that optimal usage of this model will require knowledge of all communication links within a given network, implying that centralized network planning will be required. However, in this paper, focus is on quantifying the nonlinear effects and we plan to study the design and implementation of planning algorithms in later work.

The GN model provides a tool to approach the question of how to find a nonlinear optical network model. This model has no free parameters that need precalculation but unfortunately, the GN model is also too computationally complex. The very recently suggested improved GN model, called the *enhanced GN model* [13], is even more accurate but also more complex

Manuscript received July ?, 2014; revised ???.

Pontus Johannisson is with the Photonics Laboratory, Department of Microtechnology and Nanoscience, Chalmers University of Technology, SE-412 96 Gothenburg, Sweden.

Erik Agrell is with the Communication Systems Group, Department of Signals and Systems, Chalmers University of Technology, SE-412 96 Gothenburg, Sweden.

and we will therefore not attempt to use it here. Instead, in this paper, we start from a description of how a model suitable for network optimization can be formulated and derive such a model from the GN model.

Prior to the GN model, a model for OFDM-based communication was published [14]. These two models share many features and, in fact, become identical under certain assumptions. The original model has been generalized [15] and modified to allow prediction of signal distortion in a networking context [16], and we will refer to this network model as the *OFDM model*. We compare the OFDM model with the one suggested here, and find that the OFDM model is less general due to a number of assumptions that can be relaxed.

The organization of this paper is as follows. In Sec. II, the problem is formulated and the approach is outlined. The main assumptions and approximations are given in Sec. III. The model for a multichannel fiber span is derived in Sec. IV, and it is expanded into a network model in Sec. V. After a discussion about the validity of the model assumptions in Sec. VI, an analytical and numerical comparison is made with the previously published OFDM model [16] in Sec. VII. Then, the paper is concluded.

II. Problem Statement

A. Network Topology and Terminology

A network consists of a number of *nodes*, each containing transceivers and/or routing hardware components, connected by optical communication *links*. Each link consists of N concatenated *fiber spans,* which each consists of an optical fiber followed by an erbium-doped fiber amplifier (EDFA)[1]. Each link can transmit M simultaneous *channels* using WDM.

In such a network, a large number of *connections* are established between transceivers. For each connection there is a *route,* i.e., a set of fiber links that connect the transmitting and receiving nodes via a number of intermediate nodes. We consider an all-optical network, implying that the signal is in the optical domain throughout the path. The intermediate nodes typically consist of reconfigurable add/drop multiplexers and may, in principle, include optical wavelength conversion. However, it is assumed that the OSNR penalty from this operation is then negligible.

B. Signal Degrading Mechanisms

For any connection through the network, there will be signal degradation caused by a number of mechanisms. The two most fundamental ones are amplifier noise and nonlinear signal distortion due to the Kerr nonlinearity. While the amplified spontaneous emission from optical amplifiers is easy to model, the latter presents a big challenge. Additional degrading effects include the finite signal-to-noise ratio (SNR) already at the transmitter, which may be important for large quadrature amplitude modulation constellations, and the crosstalk between different WDM channels in routing components and in the receiver. However, the efforts to increase the spectral efficiency have led to sophisticated shaping of the optical spectrum. Techniques such as orthogonal frequency-division multiplexing and Nyquist WDM have demonstrated optical signal spectra that are very close to rectangular [17]. Using a DSP filter, the channel crosstalk can then be very small in the receiver. Optical routing components, such as reconfigurable optical add-drop multiplexers, are more difficult to realize as the filter function is implemented in optical hardware, but the lack of WDM channel spectral overlap reduces the crosstalk also here. Signal degradation due to, e.g., polarization-mode dispersion is neglected as it is compensated for by the receiver equalizer. Thus, we here choose to focus on the nonlinear effects generated as the interplay between the Kerr nonlinearity and the chromatic dispersion, known as the nonlinear interference (NLI) within the GN model [12].

[1]While Raman amplification can be described within the GN model [12, Sec. X], it leads to the introduction of new system parameters and complicates the analytical expressions. It is outside the scope of the work presented here.

C. Modeling Aim

The aim of the modeling effort is to find an approximate quantitative model for the NLI for a large number of connections between network transceivers. For each connection there is a route, i.e., a set of fiber links that connect the transmitting and the receiving nodes via a number of intermediate nodes. Each link can transmit M WDM channels and for each channel $m = 1, \ldots, M$, the center frequency f_m, the bandwidth Δf_m, and the power P_m are chosen. This is summarized as the set of channel parameters $\mathbb{C}_m = \{f_m, \Delta f_m, P_m\}$. For a given link, the WDM channels can then be written as the set $\mathbb{W} = \{\mathbb{C}_1, \ldots, \mathbb{C}_M\}$. The physical parameters of a link are the power attenuation $\alpha(z)$, the group-velocity dispersion (GVD) $\beta_2(z)$, and the nonlinearity $\gamma(z)$. Here $z \in [0, L]$ denotes the distance from the beginning of the first fiber, where L is the total length of the link (possibly including several fiber spans). The link parameters are summarized in the set $\mathbb{L}(z) = \{\alpha(z), \beta_2(z), \gamma(z), L\}$.

Assume that there are a number of planned connections. To make sure that each transmission can succeed, the corresponding connection must satisfy the SNR requirement for the selected modulation format at the receiving node. The purpose of the proposed model is to calculate the SNR for a number of simultaneous connections in a network, given the network topology and the parameter sets $\mathbb{W}$ and $\mathbb{L}$ for every link in the network.

The total noise variance is the sum of all noise sources. We view amplifier noise as being added after the power gain in each optical amplifier with a variance related to the power gain and the amplifier noise figure [18]. The NLI is generated during the propagation through the fibers, but within the GN model, we view it as being added after the gain in the amplifier, i.e., at the same location and at the same power level as the amplifier noise.

D. Modeling Approach: The GN Model

We assume there is no periodic (hardware) compensation for chromatic dispersion, which seems to be a likely scenario for the future, and that no DSP compensation of nonlinear effects is carried out. Under these assumptions, the GN model

provides both accurate predictions and the potential to obtain a sufficiently low-complexity model. While there is still work in progress [13], [19] about the range of validity of the signal model used in the GN model [10, Eq. (3)], the agreement with simulations of the full model equations has been shown to be very good [11]. We discuss some known facts about the validity of the GN model in Sec. VI. Starting from the GN model, assumptions and approximations needed to obtain a network model are introduced in the following.

III. Network Model Derivation

A. General NLI Expression

The derivation is started from the GN model as stated in [20], where the model equation, [20, Eq. (1)], assumes polarization-multiplexed transmission. We point out that different conventions exist in the literature and the model equation used here [21, Eq. (1)] is identical to the one used for the OFDM model [22, Eq. (4)] but differs from [23, Eq. (71)] in the definition[2] of α and γ. As coherent systems typically transmit and receive the two polarization-multiplexed channels simultaneously, these are viewed as a unit. Assuming that the signal power spectral density (PSD) is equal in both polarizations, i.e., $G_x(f) = G_y(f) \equiv G(f)$, we use [20, Eqs. (26) and (27)] to obtain the NLI PSD

$$G_1^x(f) = 3 \iint |C(\nu, \nu', \nu + \nu' - f)|^2 \times G(\nu) G(\nu') G(\nu + \nu' - f)\, d\nu d\nu', \qquad (1)$$

where

$$C(\nu, \nu', \nu + \nu' - f) = \int_0^L \gamma(z) p(z) e^{-i4\pi^2(\nu - f)(\nu' - f) B_2(z)}\, dz. \qquad (2)$$

Here, G_1^x is the NLI PSD[3] in the x polarization but $G_x(f) = G_y(f)$ implies that $G_1^x(f) = G_1^y(f) \equiv G^{\text{NLI}}(f)$. The definitions for the normalized power evolution function, $p(z)$, and the accumulated dispersion, $B_2(z)$, are given in [20, Sec. II-B]. Notice that the channel parameter P_m is the power corresponding to G_x, i.e., the power *per polarization*. The third-order dispersion has been neglected as it has very small impact on the NLI [20]. Finding the NLI PSD at a given frequency involves evaluating three nested integrals. The numerical complexity of this is high, which motivates our search for analytical simplifications of this expression.

B. NLI Accumulation

The GN model was originally derived for a single link where all WDM channels propagate together from the transmitter to the receiver, but in the network model we need the capability of WDM channel switching/routing. The GN model builds on a certain signal model [10, Eq. (3)], where a fundamental assumption is that the launched signal can be written on (or, at least, quickly approaches) this form. Then, during propagation, the changes of the launched signal are accounted for by a linearized propagation equation. As the signal leaves one fiber span and enters the next, the phase relation between different frequency components is conserved and this leads to a coherent accumulation of the complex amplitude of the signal perturbation corresponding to the NLI. In a network, channels can be added or dropped, which is incompatible with the original GN model.

Poggiolini et al. have investigated the consequences from assuming that the NLI generated in different fiber spans can be added *incoherently*, i.e., that the NLI PSDs are summed instead of the corresponding complex amplitudes [12]. This assumption results in a significant analytical (and numerical) simplification, and numerical simulations have shown that the difference compared with the exact result is small. From the discussion above it is clear that in a network, the situation is neither fully coherent nor fully incoherent, but we will use the assumption that the NLI accumulates incoherently. It then becomes possible to calculate the NLI PSD generated in each channel in each fiber span separately and then sum these contributions along the entire route. Unfortunately, this assumption seems to slightly underestimate the NLI [12, Sec. IX].

For a given link, the NLI PSD $G_{\text{link}}^{\text{NLI}}(f)$ is a function of $\mathbb{L}$ and $\mathbb{W}$. The dependence on the link is static since the hardware does not change, but $G_{\text{link}}^{\text{NLI}}$ must be easy to evaluate as a function of $\mathbb{W}$. The assumption of incoherent NLI accumulation implies that we can split each link $\mathbb{L}$ into N spans $\mathbb{L}_n$, $n = 1, \ldots, N$, calculate the NLI independently for each span, and obtain the total NLI for a link from the NLI contributions from each span. In the special case that all spans are identical, it is obtained that $G_{\text{link}}^{\text{NLI}} = N G_{\text{span}}^{\text{NLI}}$ [12, Eq. (18)].

We assume that the loss of each fiber span is exactly compensated for by an EDFA placed at the end of the span. The received power is thus equal to the transmitted power P. Furthermore, since the link parameters $\mathbb{L}_n$ are assumed to be constant within a fiber span, the z dependence is dropped from now on. Without loss of generality, we will therefore calculate the NLI generated in a single fiber span in Sec. IV and then in Sec. V extend these results to the network layer.

IV. NLI for a Single Fiber Span

In this section, the NLI is derived for all channels in a single fiber span. The inputs are the channel parameters, $\mathbb{W}$, and the link parameters, $\mathbb{L}_n$. The output is the NLI PSD $G_{\text{span}}^{\text{NLI}}(f_m)$ for $m = 1, \ldots, M$. Although this case has been discussed in the literature [12], [24], we study it in detail for two reasons. First, most results in the literature are for the center channel in fixed-grid WDM transmission. However, flexible-grid WDM with flexible bandwidths and power levels [23], [25] is essential for a complete network model. Second, we find it useful to summarize all calculations in a consistent notation to make this document self-contained.

[2]To convert the expressions given here to the ones given (for polarization-multiplexed transmission) in [12], the following must be carried out: The attenuation is defined in [12] using the amplitude, not the power, implying that α must be replaced by 2α. The nonlinear parameter in [12] does not contain the factor $8/9$ [11, Appendix D], implying that γ must be replaced by $8\gamma/9$.

[3]The subscript "1" in the NLI PSD indicates that the result comes from a first-order perturbation analysis.

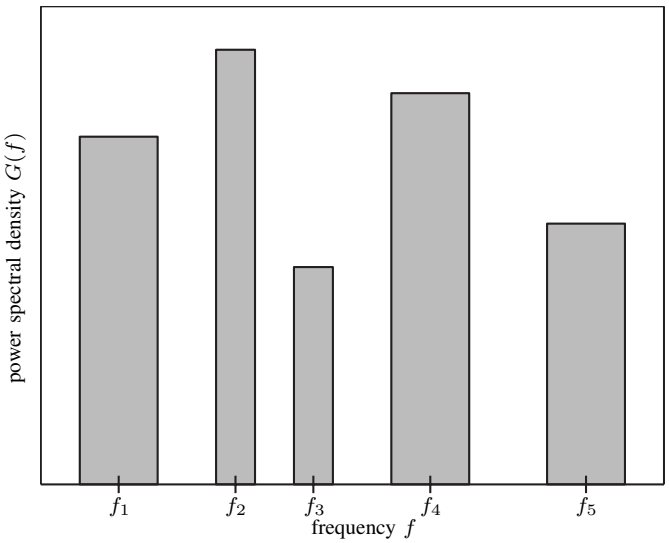

Fig. 1. The PSD of a flexible-grid example WDM system, representing a set of $M = 5$ channels with different center frequencies, bandwidths, and powers.

As seen from (1), the signal PSD for each individual WDM channel must be known. The exact shape depends on the transmitter, but as mentioned, much effort is currently spent on making the optical signal spectra close to rectangular [17]. Since this shape leads to improved spectral efficiency and also creates minimal channel crosstalk, it is likely that signals in future systems will approximate this shape. Thus, we assume that each channel spectrum is rectangular, which implies that the channel PSD is completely specified by $\mathbb{C}_m$ as $G(f_m) = P_m/\Delta f_m$. The channel PSDs may have different center frequencies, bandwidths, and powers, as exemplified in Fig. 1.

From (1) and (2), the NLI is

$$G_{\text{span}}^{\text{NLI}}(f) = \iint \frac{3\gamma^2 G(\nu)G(\nu')G(\nu+\nu'-f)}{\alpha^2 + 16\pi^4\beta_2^2(\nu-f)^2(\nu'-f)^2}\, d\nu d\nu', \quad (3)$$

where $1 - e^{-(\alpha+i4\pi^2\beta_2(\nu-f)(\nu'-f))L} \approx 1$ was used. This approximation is accurate for a fiber loss of 7 dB or more [12, Sec. XI-A]. The NLI is frequency-dependent and the channel $\mathbb{C}_m$ is affected by the amount of NLI that passes the corresponding receiver filter. Due to the assumption about the signal PSD shape, the matched filter has a rectangular frequency response. As it is difficult to analytically account for the variation of $G_{\text{span}}^{\text{NLI}}(f)$ within a channel, we assume that the NLI variance for channel $\mathbb{C}_m$ can be approximated as $G_{\text{span}}^{\text{NLI}}(f_m)\,\Delta f_m$, i.e., that it can be based on the value at the center frequency of each channel. This is a good approximation, as the NLI varies slowly within a given channel see, e.g., [12, Fig. 5] and [20, Fig. 1]. Furthermore, this assumption is conservative in the sense that it typically leads to a slight overestimation of the NLI.

A. Approximate Integration

The next step is to find an approximate value for $G_{\text{span}}^{\text{NLI}}(f_m)$ for channel m. This is done by generalizing the approach previously used for the center channel [12], [26]. Calculations using a similar approach can be found in [23, Sec. V] and have also been applied to network modeling very recently [25]. As seen in (3), the integration is over the entire $\nu \times \nu'$ plane, but the integrand is nonzero only within distinct regions determined by the product of the PSDs. To exemplify, we consider channel $m = 2$ in the set of WDM channels in Fig. 1. The PSD product in (3) is a piecewise constant function that is illustrated in the $\nu\times\nu'$ plane in Fig. 2 by the dark gray regions. The vertical, horizontal, and diagonal regions illustrate $G(\nu)$, $G(\nu')$, and $G(\nu+\nu'-f_m)$, respectively. The product of the PSDs is nonzero only where three regions overlap. It is seen that this corresponds to polygons of different shapes, making exact integration difficult. The integrand weight function

$$w_m(\nu,\nu') = \frac{3\gamma^2}{\alpha^2 + 16\pi^4\beta_2^2(\nu-f_m)^2(\nu'-f_m)^2} \quad (4)$$

is illustrated by the colored contours and in order to discuss its properties we introduce

$$\eta_m = \frac{w(f_m+\Delta f_m/2, f_m+\Delta f_m/2)}{w(f_m,f_m)} = \left(1+\frac{\pi^4\beta_2^2\Delta f_m^4}{\alpha^2}\right)^{-1}. \quad (5)$$

In this way, η_m is the fraction of the weight function evaluated at the edge of the mth channel spectrum relative to its channel center frequency. Using a dispersion parameter $D = 16$ ps/(nm km) and power attenuation $\alpha = 0.2$ dB/km, we find $\eta_m \approx 0.84$ for a 10 GHz channel and $\eta_m \approx 0.078$ for a 28 GHz channel. When the values of $|\nu - f_m|$ and $|\nu' - f_m|$ are increased, w_m decreases rapidly.

We proceed by assuming that (i) only the polygons containing $\nu = f_m$ or $\nu' = f_m$ need to be included and (ii) each polygon can be approximated by a rectangle of minimal area that contains the polygon. The first of these assumptions is equivalent to including *self-channel interference* (SCI), represented by the single polygon that surrounds $(\nu,\nu') = (f_m, f_m)$, and *cross-channel interference* (XCI). A similar approximation was discussed and illustrated in [12, Fig. 3] for the center channel when the channels have equal bandwidths and spacing. This approximation typically leads to a very small error, since w_m is negligible elsewhere. The second assumption leads to an overestimation of the NLI. For example, in the SCI case, the polygon area is extended by a factor $4/3$, but the effect from this is reduced since w_m is highest in the center. As shown above, this has some impact on the result for narrow-band channels. Improvements of this approximation are possible, for example following [26], but here the simple and conservative assumption above is used.

Inspection of (3) shows that the result is unchanged if ν and ν' are substituted for each other, which in Fig. 2 corresponds to mirroring the entire integration domain in the line $\nu = \nu'$. Thus, evaluating the NLI for channel m, the total NLI can be written as

$$G_{\text{span}}^{\text{NLI}}(f_m) = G_m^{\text{SCI}} + \sum_{\substack{m'=1 \\ m'\neq m}}^{M} G_{mm'}^{\text{XCI}}, \quad (6)$$

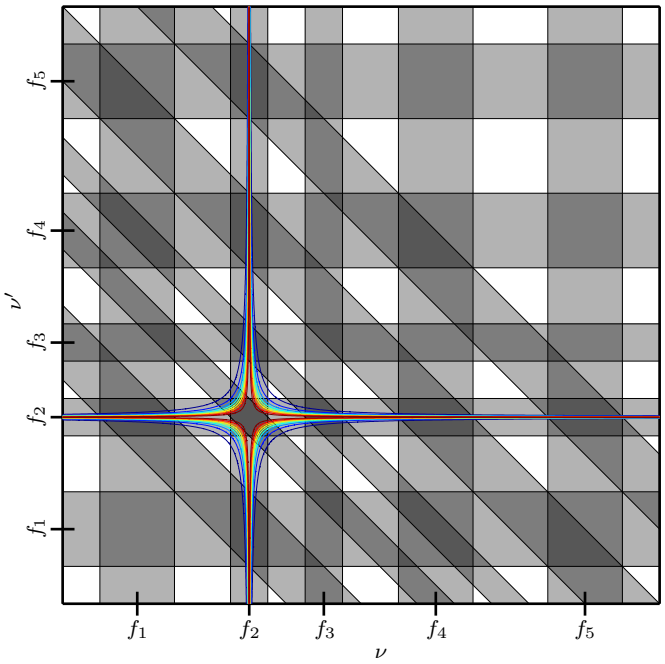

Fig. 2. In this visual representation of (3), the vertical, horizontal, and diagonal shaded regions correspond to $G(\nu)$, $G(\nu')$, and $G(\nu+\nu'-f)$, respectively, where we choose $f=f_2$. This illustrates the qualitative behavior of the numerator in (3) for the example WDM channels in Fig. 1. Only the intersections of these regions contribute to the integral. The contours show the weight function from (4), supporting the notion of considering only the regions containing $\nu=f_m$ or $\nu'=f_m$.

where

$$G_m^{\text{SCI}} = \iint_{\Omega_{mm}} w_m(\nu,\nu')G^3(f_m)\,d\nu d\nu', \tag{7}$$

$$G_{mm'}^{\text{XCI}} = 2\iint_{\Omega_{mm'}} w_m(\nu,\nu')G(f_m)G^2(f_{m'})\,d\nu d\nu', \tag{8}$$

and the integration domain $\Omega_{mm'}$ is the rectangle $\nu\in[f_m-\Delta f_m/2, f_m+\Delta f_m/2]$, $\nu'\in[f_{m'}-\Delta f_{m'}/2, f_{m'}+\Delta f_{m'}/2]$. By introducing

$$\xi = \frac{4\pi^2|\beta_2|}{\alpha} \tag{9}$$

and

$$F_{mm'}^2 = \iint_{\Omega_{mm'}} \frac{1}{1+\xi^2(\nu-f_m)^2(\nu'-f_{m'})^2}d\nu d\nu', \tag{10}$$

it follows that

$$G_{\text{span}}^{\text{NLI}}(f_m) = \frac{3\gamma^2}{\alpha^2}F_{mm}^2G^3(f_m) + \sum_{\substack{m'=1\\m'\neq m}}^{M}\frac{6\gamma^2}{\alpha^2}F_{mm'}^2G(f_m)G^2(f_{m'}). \tag{11}$$

Unfortunately, the exact result for $F_{mm'}^2$ has to be expressed in terms of the dilog function, which is defined in terms of a power series as $\text{Li}_2(z)=\sum_{n=1}^{\infty}z^n/n^2$. (Outside the unit circle, i.e., at $|z|>1$, analytic continuation is used to extend the definition.) For notational convenience, we introduce

$$x_1 = \frac{\Delta f_m}{2}\left(f_m - f_{m'} + \frac{\Delta f_{m'}}{2}\right)\xi, \tag{12}$$

$$x_2 = \frac{\Delta f_m}{2}\left(f_{m'} - f_m + \frac{\Delta f_{m'}}{2}\right)\xi \tag{13}$$

to write (10) as

$$F_{mm'}^2 = \frac{i}{\xi}[\text{Li}_2(-ix_1) - \text{Li}_2(ix_1) + \text{Li}_2(-ix_2) - \text{Li}_2(ix_2)]. \tag{14}$$

From this expression, it is not obvious that $F_{mm'}^2$ is a real quantity. However, $\text{Li}_2(z^*)=[\text{Li}_2(z)]^*$, where $*$ denotes complex conjugation and z is an arbitrary complex number, and this allows us to obtain

$$F_{mm'}^2 = \frac{2}{\xi}\{\text{Im}[\text{Li}_2(ix_1)] + \text{Im}[\text{Li}_2(ix_2)]\}, \tag{15}$$

where $\text{Im}(\cdot)$ denotes the imaginary part. Using (15) together with (11), the model is complete.

B. Further Simplification

The result above has been presented in terms of the special function Li_2. In order to obtain a simple and intuitive expression, we approximate one step further. This is done using an asymptotic expansion of the dilog function, but an alternative way is to use the inverse hyperbolic sine function, see, e.g., [12, Eq. (40)]. The asymptotic expansion leads to the simplest expression, but if maximum accuracy is the objective, we suggest using (15). Using the result from Appendix A, (11) can be written as

$$G_{\text{span}}^{\text{NLI}}(f_m) = \frac{3\gamma^2G(f_m)}{2\pi\alpha|\beta_2|}\left[G^2(f_m)\ln\left|\frac{\pi^2\beta_2(\Delta f_m)^2}{\alpha}\right| + \sum_{\substack{m'=1\\m'\neq m}}^{M}G^2(f_{m'})\ln\left(\frac{f_{mm'}+\Delta f_{m'}/2}{f_{mm'}-\Delta f_{m'}/2}\right)\right], \tag{16}$$

where we introduced $f_{mm'}\equiv|f_m-f_{m'}|$. As shown in Appendix A, the asymptotic expansion is not accurate for channels with a bandwidth below 28 GHz. Further information about the GN model when using rectangular channel spectra can be found in [24], where a similar XCI expression is given in Eq. (20).[4]

V. Summary of the Network Model

We are now ready to summarize the model and extend it to a network of multiple spans and links. The description in this section is intended to be self-contained and can be implemented without studying the details of the derivation in previous sections. It is evaluated in two stages; first to evaluate the channel quality of every *link* in the network, and second, to evaluate the quality of every *connection*.

The first stage utilizes the following inputs for a given link, denoted by l, in the network:

[4]There is a typographical error in [24, Eq. (20)]: "ln" is missing before the square bracket.

- The link parameters $\mathbb{L}_n$ of every fiber span $n = 1, \ldots, N$. These are assumed to be the same for all channels.
- The (constant) PSD G^{ASE} of the amplifier noise. It is equal to the sum of the noise PSDs added by the amplifier in each span, which are given by the amplifier gains and noise figures [18].
- The channel parameters $\mathbb{C}_m$ for $m = 1, \ldots, M$. These are assumed to be constant through all fiber spans.

Given these quantities, the model is evaluated as follows:

1) Calculate $G(f_m) = P_m/\Delta f_m$ for $m = 1, \ldots, M$.
2) For $n = 1, \ldots, N$ and $m = 1, \ldots, M$, use $\mathbb{L}_n$ to evaluate (11), where $F^2_{mm'}$ is given by (15). Denote the PSD $G^{\text{NLI}}_{\text{span}}(f_m)$ returned by (11) by G^{NLI}_{mn}.
3) For $m = 1, \ldots, M$, calculate the SNR as $SNR_{lm} = P_m/\sigma^2_m$, where

$$\sigma^2_m = \Delta f_m \left(G^{\text{ASE}} + \sum_{n=1}^{N} G^{\text{NLI}}_{mn} \right) \tag{17}$$

represents the total linear and nonlinear noise contributions.

This is repeated for every link l in the network. Alternatively, (11) and (15) may be replaced by (16).

In the second stage, the SNR of an arbitrary connection in the network is calculated. The network is all-optical and assuming no format conversion, the bandwidth Δf_m is constant for all links in the connection. The center frequency f_m may change if optical wavelength conversion is performed, but any performance penalty from this has been neglected. The power P_m is constant, as we have assumed the gains to balance the losses. However, our model holds also if P_m changes between the links in a route, if the noise added in this process is negligible compared to the total G^{ASE}.

The input to the second stage can be represented as follows.

- The route of the connection, represented as K link assignments $l = l_1, \ldots, l_K$ and channel assignments $m = m_1, \ldots, m_K$.
- The link and channel SNRs SNR_{lm} obtained from the first stage above.

Based on this input, the SNR of the connection under consideration is finally obtained as

$$SNR = \left(\sum_{k=1}^{K} \frac{1}{SNR_{l_k m_k}} \right)^{-1}. \tag{18}$$

VI. Discussion

The described model is simple enough to allow optimization of optical networks operating in the nonlinear regime. As has been made clear in the derivation, a number of assumptions and approximations have been introduced. We will here discuss the model accuracy.

First, the model obviously relies on the GN model and already (1) and (2) are approximate expressions relying on the perturbation approach and the signal model assumption [27]. A fundamental assumption is that the dispersive effects are strong and the GN model should not be used in systems with periodic dispersion compensation. Nevertheless, the initial part of a system, where the accumulated dispersion is still small, has some impact on the accuracy [28]. Furthermore, the signal bandwidth should be sufficiently large and this means that single-channel transmission is less accurately modeled. While these assumptions are likely to be compatible with future optical networks, there are some further questions about the model validity. For example, it is a surprising fact that the model has no dependence on the choice of modulation format [13], [19]. The discussion about the validity of the GN model is ongoing.

The assumption about incoherent noise accumulation has been investigated in the literature and it is known that the special case expression from Sec. III-B is more accurately written as $G^{\text{NLI}}_{\text{link}} = N^{1+\epsilon} G^{\text{NLI}}_{\text{span}}$, where $\epsilon \in [0, 1]$ depends on both the signal and the system [12, Sec. IX]. The drawback of this approach is that spans in the links are then assumed to be identical. However, in many practical cases, $\epsilon \ll 1$. This has been found theoretically [29, Sec. III-C], but there are also experimental investigations that indicate a higher value of ϵ [30].

Finally, approximations were introduced in the integration of (3). As seen, the value of w_m is quickly reduced as the frequency separation is increased. Thus we expect the choice to include only SCI and XCI to lead to a small error, as long as not too narrow channel bandwidths are considered, but this is, as discussed above, also an inherent assumption of the GN model. For the same reason, the error introduced by approximating the integration polygons by rectangles is small.

In summary, the network model presented here is not universally applicable due to the various assumptions specified above. Nevertheless, the model combines low computational complexity with reasonable accuracy and, as will be showed in the next Section, constitutes a considerable step forward in terms of accuracy compared to the OFDM model [16]. Further accuracy improvements may be possible, e.g., by using a more accurate model [13] and/or more accurate approximations. Another path is to exploit semi-analytical methods, e.g., as suggested in [9]. We will leave such improvements for later study.

VII. Comparison with the OFDM Model

The expression in [16, Eq. (3)] is somewhat similar to the simplified expression given in (16) above. However, there are a number of differences and the network model reported here is more general. To see this, the relation between the two underlying models is first discussed and then the two network models are compared numerically for a number of selected signal PSDs.

A. Assumptions in the Two Models

The derivation of the OFDM model in [16] is found in [16, Appendix A] and starts from the first five equations in [15]. This expression is already similar to the corresponding one for the GN model, see, e.g., [20, Eq. (31)]. However, it is directly seen that the PSD of the NLI of [16], which is denoted by I_{NL}, has no frequency dependence. Instead, it refers to a special case of the GN model obtained by setting $f = 0$, i.e.,

evaluating at the center frequency of the optical spectrum. The OFDM model further assumes that the loss in each fiber is sufficiently large, just as described after (3) above. Finally, the OFDM model assumes that the signal PSD is equal in all channels, which has the effect that the signal PSD, denoted by I, is outside the sums in [16, Eq. (3)]. In order to compare the models, we modify [20, Eq. (31)] by evaluating at $f = 0$ and setting all PSDs to be equal. The algebraic manipulations are very simple and will not be given here. We also rewrite the OFDM-based expression in [16, Appendix A] by inserting the definitions of f_{PA} and f_w [16, p. 3045].

The resulting expressions for I_{NL} and G^{NLI} now differ in three ways. First, $I_{\mathrm{NL}} = 2G^{\mathrm{NLI}}/3$, which is due to the assumption of single-polarization transmission in [15, Sec. II].[5] While this is easy to adjust, there is also the second assumption that the spectrum is symmetric around $f = 0$. Thus, the sum in [16, Eq. (3)] is only for $n = 1, 2, \ldots, N$, although there are $2N+1$ channels. This reduces the generality of the result. Third, the integration domains for the two integrals are different; G^{NLI} results from integration over a polygon-shaped domain, while I_{NL} is obtained by integrating over a quadratic area in the $f \times f_1$-plane. The approximation of the integration domain for G^{NLI} in Sec. IV-A however makes the integration domains identical, but the assumption of a symmetric spectrum is never done for G^{NLI}.

There is one further important comment that must be made about the two underlying expressions. As pointed out in [20, Sec. V], the "phase-array factor", i.e., the ratio between two sinusoidal functions, e.g., in [15, Eq. (5)] requires the assumption that all fibers have identical parameters, including the length. This may not be the case in practice and this assumption has not been made in the model presented here. Instead, the assumption has been made that there is no correlation between the NLI generated in different fibers. It is known that this is a good approximation, see, e.g., the comprehensive discussion about coherent/incoherent accumulation of NLI in [12]. At any rate, accounting for a general phase-array factor analytically is difficult and it may be unavoidable to resort to numerical approaches if this is necessary to include, see, e.g., [9]. For this reason, we have compared the two models for a single span of fiber below.

B. Numerical Comparison of the Two Models

Since the two models share the underlying theory, we here compare the model results with numerical simulations of the exact expression that the two models strive to approximate.

In the first case, we have selected a WDM signal with $M = 21$ channels placed symmetrically around $f = 0$. The symbol rate is 28 GBd for each channel and channel separations equal to 28 GHz (Nyquist WDM), 50 GHz, and 100 GHz have been investigated. The link parameters used in Figs. 3 and 4 are: power attenuation $\alpha = 0.2$ dB/km, GVD parameter β_2 calculated from the dispersion parameter $D = 16$ ps/(nm km), nonlinear parameter $\gamma = 1.3$ W^{-1}km^{-1},

[5]Polarization-multiplexed transmission has been investigated in [22] using exactly the same modeling equation as in [20].

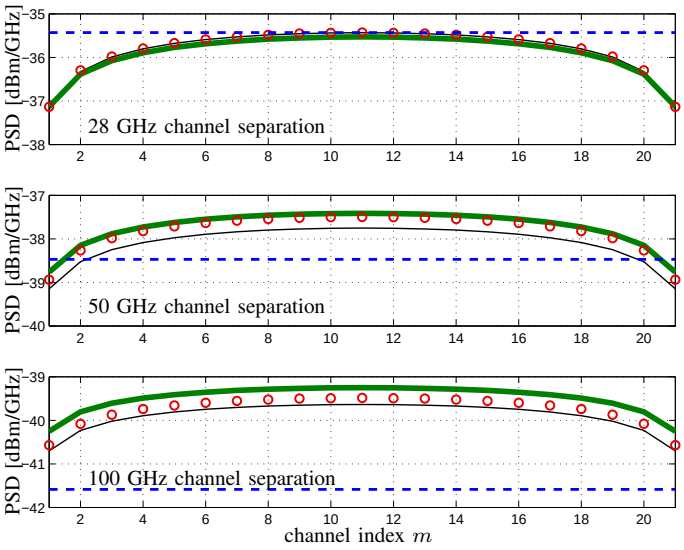

Fig. 3. The NLI PSD calculated at the channel center frequencies of each of the 21 WDM channels. Black thin solid line: Numerical integration. Green thick solid line: dilog results. Red circles: log results. Blue thin dashed line: OFDM model.

and fiber length $L = 80$ km. The power per channel and polarization is $P_m = 0$ dBm.

The results for this case are seen in Fig. 3. The horizontal axes show the channel index, m, which runs from 1 to 21. The vertical axes show the NLI PSD in the center of each channel and the three plots in Fig. 3 are for different channel separations. The black thin solid lines (partially obscured) are the results from numerical integration of (3). As expected, the channels closer to the edge of the WDM spectrum are less affected, i.e., the NLI decreases with increasing separation from the center channel. The green thick solid lines and the red circles show the results from (11) when using (14) and (25), respectively. For convenience, these are called the "dilog results" and "log results". As long as MCI can be neglected, the dilog results consistently overestimate the NLI. This is due to the conservative approach above to approximate the polygons by rectangles. As a matter of fact, the log results are consistently more accurate in Fig. 3, which is because the logarithmic asymptotic expansion consistently underestimates the dilog function. The overestimation in the dilog result is everywhere below 0.5 dB in Fig. 3.

The blue dashed lines show the OFDM model for comparison. The ceiling function, $\lceil \cdot \rceil$, is used in [16, Eq. (3)] and this introduces a problem. As $2\pi f_{PA}^2 \approx 10^{20}$ GHz^2, the numerator and denominator will evaluate to the same value and $I_{NL} = 0$. We have solved this by using the exact expression from [15, Eq. (14)], which is applicable in the case selected here. It is seen that the result is very accurate for the center channel in the Nyquist WDM case. However, the OFDM model does not account for the differences in NLI in the different channels and the estimate is less accurate for the edge channels. For the non-Nyquist WDM cases, the OFDM model underestimates the center channel NLI. As the underestimation is significant, we have investigated the OFDM expression for the case with

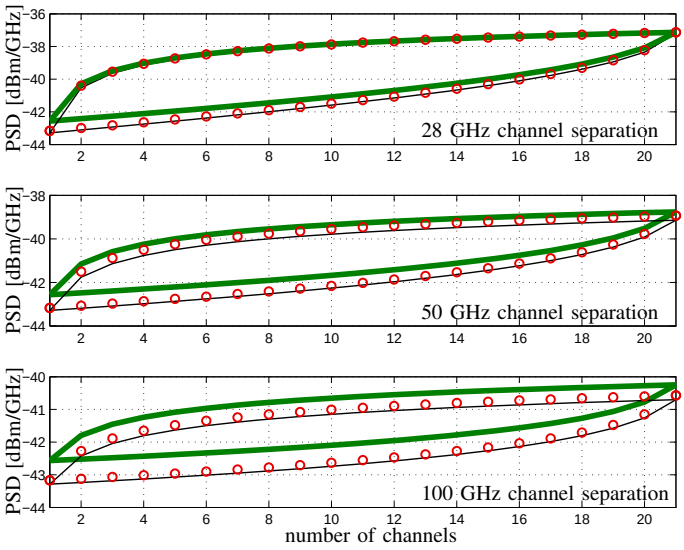

Fig. 4. The NLI PSD calculated at the center frequency of the channel at the edge of the WDM spectrum. Upper set of curves in each figure: Adding neigboring WDM channels. Lower set of curves in each figure: Adding WDM channels from the other edge of the WDM spectrum. Line types have identical meaning as in Fig. 3. The OFDM model has not been included as it gives no prediction for an asymmetric WDM spectrum.

100 GHz channel separation. The main difference comes from the term $(1-\Delta G/\Delta B)$ in [15, Eq. (14)], where ΔG is the guard band and ΔB is the channel separation. This evaluates to 0.28, or -5.5 dB. In the last factor in [15, Eq. (14)], B, i.e., the total bandwidth, increases but the net effect is a further decrease of the estimate due to the second term. We conclude that the 6.2 dB decrease in NLI seen in Fig. 3 when changing the channel spacing from 28 GHz to 100 GHz is the prediction given by [15].

We have further investigated a case where the WDM channel spectrum is not symmetric around the center channel. This is incompatible with one of the assumptions of the OFDM model, which implies that we cannot perform a comparison in this case. The numerical and analytical results are indicated in Fig. 4, where the three different plots are again for different channel separations. In this figure, all NLI PSD values are for the channel with $m=1$, i.e., at the edge of the WDM spectrum, and the horizontal axes show the total number of channels. Thus, the leftmost value is for a single channel and the rightmost value is for 21 channels as in Fig. 3. (This implies that the rightmost values are included also in Fig. 3.) The upper set of curves is obtained by filling the WDM spectrum by introducing channels directly neighboring to the channel under study, i.e., the channels with $m=2,3,4,\ldots$ in Fig. 3. The lower curve corresponds to filling the WDM spectrum in the opposite direction, introducing the channels with $m=21,20,19,\ldots$ in Fig. 3. As an example, three channels would then mean including the channel under study and two channels in the frequency slots with the largest possible frequency separation.

In this way, the separation between the two sets of curves gives an indication of the difference in impact from close and distant neighboring WDM channels. Again it is seen that the dilog result consistently overestimates the NLI, in some cases with 100 GHz channel separation up to 0.7 dB. However, the log results are again more accurate due to the partial cancellation from two different error sources. From the result we conclude that, in particular for small channel spacing, the difference in NLI can be substantial depending on the placement of the neighboring channels. This effect is neglected in the OFDM model.

VIII. Conclusion

Starting from the Gaussian noise model, a low-complexity model for signal quality prediction in a nonlinear fiber-optic network has been presented. Comparing the model with numerical results we find that the NLI is estimated in a conservative way, i.e., the NLI is slightly overestimated. Comparing with a previously suggested OFDM-based model we conclude that the model presented here is more general. The center frequencies, bandwidths, and transmit powers can be chosen independently for each WDM channel, and the here presented model accurately accounts for that fact that the NLI is different for different channels in the WDM spectrum.

Appendix A
Asymptotic Expansion

For $|z|\gg 1$, the dilog function has the asymptotic expansion

$$\mathrm{Li}_2(z)=\sum_{k=0}^{\infty}(-1)^k(1-2^{1-2k})(2\pi)^{2k}\frac{B_{2k}}{(2k)!}\frac{[\ln(-z)]^{2-2k}}{\Gamma(3-2k)}, \tag{19}$$

where B_{2k} are the Bernoulli numbers. As the $\Gamma(z)$ function is not defined for negative integers, there are only two terms in the expansion, giving asymptotically

$$\mathrm{Li}_2(z)=-\frac{\pi^2}{6}-\frac{1}{2}\ln^2(-z). \tag{20}$$

However, assuming $x\in\mathbb{R}$, we have

$$\ln(ix)=\ln|x|+i\arg(ix)=\ln|x|+s_x i\frac{\pi}{2}, \tag{21}$$

$$\ln(-ix)=\ln|x|+i\arg(-ix)=\ln|x|-s_x i\frac{\pi}{2}, \tag{22}$$

where s_x is the sign of x. We get

$$\begin{aligned}\mathrm{Li}_2(ix)&=-\frac{\pi^2}{6}-\frac{1}{2}\left(\ln|x|-s_x i\frac{\pi}{2}\right)^2\\&=-\frac{1}{2}\ln^2|x|+s_x i\frac{\pi}{2}\ln|x|-\frac{\pi^2}{24}\end{aligned} \tag{23}$$

and

$$\mathrm{Li}_2(-ix)=-\frac{1}{2}\ln^2|x|-s_x i\frac{\pi}{2}\ln|x|-\frac{\pi^2}{24}, \tag{24}$$

which gives

$$F^2_{mm'}=\frac{\pi}{\xi}(s_{x_1}\ln|x_1|+s_{x_2}\ln|x_2|). \tag{25}$$

The condition $|z|\gg 1$ is most critical for the SCI term, where $|z|=|x_1|=|x_2|=|(\Delta f_m)^2\xi/4|=\pi^2(\Delta f_m)^2|\beta_2|/\alpha$. Using the same parameters as in Sec. IV-A, this evaluates to 3.4 for a 28 GHz channel. At this value the asymptotic expansion is 13 % below the exact value, showing that the asymptotic expansion should not be used for more narrow channels.

REFERENCES

[1] R.-J. Essiambre and R. W. Tkach, "Capacity trends and limits of optical communication networks," *Proc. IEEE*, vol. 100, no. 5, pp. 1035–1055, May 2012.

[2] I. de Miguel, R. J. Durán, R. M. Lorenzo, A. Caballero, I. Tafur Monroy, Y. Ye, A. Tymecki, I. Tomkos, M. Angelou, D. Klonidis, A. Francescon, D. Siracusa, and E. Salvadori, "Cognitive dynamic optical networks," in *Optical Fiber Communication Conference (OFC)*, 2013, p. OW1H.1.

[3] O. Rival and A. Morea, "Cost-efficiency of mixed 10-40-100Gb/s networks and elastic optical networks," in *Optical Fiber Communication Conference (OFC)*, 2011, p. OTuI4.

[4] O. Gerstel, M. Jinno, A. Lord, and S. J. Ben Yoo, "Elastic optical networking: A new dawn for the optical layer?" *IEEE Comm. Mag.*, vol. 50, no. 2, pp. S12–S20, Feb. 2012.

[5] R. Ramaswami and K. N. Sivarajan, "Routing and wavelength assignment in all-optical networks," *IEEE/ACM Transactions on Networking*, vol. 3, no. 5, pp. 489–500, Oct. 1995.

[6] H. Zang, J. P. Jue, and B. Mukherjee, "A review of routing and wavelength assignment approaches for wavelength-routed optical WDM networks," *Optical Networks Magazine*, pp. 47–60, Jan. 2000.

[7] S. Azodolmolky, M. Klinkowski, E. Marin, D. Careglio, J. S. Pareta, and I. Tomkos, "A survey on physical layer impairments aware routing and wavelength assignment algorithms in optical networks," *Elsevier Computer Networks*, vol. 53, no. 7, pp. 926–944, May 2009.

[8] B. Garcia-Manrubia, P. Pavon-Marino, R. Aparicio-Pardo, M. Klinkowski, and D. Careglio, "Offline impairment-aware RWA and regenerator placement in translucent optical networks," *J. Lightw. Technol.*, vol. 29, no. 3, pp. 265–277, Feb. 2011.

[9] E. Seve, P. Ramantanis, J.-C. Antona, E. Grellier, O. Rival, F. Vacondio, and S. Bigo, "Semi-analytical model for the performance estimation of 100Gb/s PDM-QPSK optical transmission systems without inline dispersion compensation and mixed fiber types," in *European Conference on Optical Communication (ECOC)*, 2013, p. Th.1.D.2.

[10] P. Poggiolini, A. Carena, V. Curri, G. Bosco, and F. Forghieri, "Analytical modeling of nonlinear propagation in uncompensated optical transmission links," *IEEE Photon. Technol. Lett.*, vol. 23, no. 11, pp. 742–744, Jun. 2011.

[11] A. Carena, V. Curri, G. Bosco, P. Poggiolini, and F. Forghieri, "Modeling of the impact of nonlinear propagation effects in uncompensated optical coherent transmission links," *J. Lightw. Technol.*, vol. 30, no. 10, pp. 1524–1539, May 2012.

[12] P. Poggiolini, "The GN model of non-linear propagation in uncompensated coherent optical systems," *J. Lightw. Technol.*, vol. 30, no. 24, pp. 3857–3879, Dec. 2012.

[13] A. Carena, G. Bosco, V. Curri, Y. Jiang, P. Poggiolini, and F. Forghieri, "EGN model of non-linear fiber propagation," *Opt. Express*, vol. 22, no. 13, pp. 16 335–16 362, Jun. 2014.

[14] X. Chen and W. Shieh, "Closed-form expressions for nonlinear transmission performance of densely spaced coherent optical OFDM systems," *Opt. Express*, vol. 18, no. 18, pp. 19 039–19 054, Aug. 2010.

[15] G. Gao, X. Chen, and W. Shieh, "Analytical expressions for nonlinear transmission performance of coherent optical OFDM systems with frequency guard band," *J. Lightw. Technol.*, vol. 30, no. 15, pp. 2447–2454, Aug. 2012.

[16] H. Beyranvand and J. A. Salehi, "A quality-of-transmission aware dynamic routing and spectrum assignment scheme for future elastic optical networks," *J. Lightw. Technol.*, vol. 31, no. 18, pp. 3043–3054, Sep. 2013.

[17] R. Schmogrow, M. Winter, M. Meyer, D. Hillerkuss, S. Wolf, B. Baeuerle, A. Ludwig, B. Nebendahl, S. Ben-Ezra, J. Meyer, M. Dreschmann, M. Huebner, J. Becker, C. Koos, W. Freude, and J. Leuthold, "Real-time Nyquist pulse generation beyond 100 Gbit/s and its relation to OFDM," *Opt. Express*, vol. 20, no. 1, pp. 317–337, Jan. 2011.

[18] G. P. Agrawal, *Fiber-Optic Communication Systems*, 4th ed. John Wiley & Sons, 2010.

[19] R. Dar, M. Feder, A. Mecozzi, and M. Shtaif, "Properties of nonlinear noise in long, dispersion-uncompensated fiber links," *Opt. Express*, vol. 21, no. 22, pp. 25 685–25 699, Oct. 2013.

[20] P. Johannisson and M. Karlsson, "Perturbation analysis of nonlinear propagation in a strongly dispersive optical communication system," *J. Lightw. Technol.*, vol. 31, no. 8, pp. 1273–1282, Apr. 2013.

[21] D. Wang and C. R. Menyuk, "Polarization evolution due to the Kerr nonlinearity and chromatic dispersion," *J. Lightw. Technol.*, vol. 17, no. 12, pp. 2520–2529, Dec. 1999.

[22] W. Shieh and X. Chen, "Information spectral efficiency and launch power density limits due to fiber nonlinearity for coherent optical OFDM systems," *IEEE Photon. J.*, vol. 3, no. 2, pp. 158–173, Apr. 2011.

[23] P. Poggiolini, G. Bosco, A. Carena, V. Curri, Y. Jiang, and F. Forghieri, "A detailed analytical derivation of the GN model of non-linear interference in coherent optical transmission systems," *arXiv:1209.0394v13 [physics.optics]*, 2014.

[24] A. Bononi, O. Beucher, and P. Serena, "Single- and cross-channel nonlinear interference in the Gaussian Noise model with rectangular spectra," *Opt. Express*, vol. 21, no. 26, pp. 32 254–32 268, Dec. 2013.

[25] A. Bononi, P. Serena, G. Picchi, and A. Morea, "Load-aware transparent reach maximization in flexible optical networks," in *European Conference on Networks and Optical Communications (NOC)*, 2014, pp. 165–172.

[26] S. J. Savory, "Approximations for the nonlinear self-channel interference of channels with rectangular spectra," *IEEE Photon. Technol. Lett.*, vol. 25, no. 10, pp. 961–964, May 2013.

[27] P. Serena and A. Bononi, "On the accuracy of the Gaussian nonlinear model for dispersion-unmanaged coherent links," in *European Conference on Optical Communication (ECOC)*, 2013, p. Th.1.D.3.

[28] A. Carena, G. Bosco, V. Curri, P. Poggiolini, and F. Forghieri, "Impact of the transmitted signal initial dispersion transient on the accuracy of the GN-model of non-linear propagation," in *European Conference on Optical Communication (ECOC)*, 2013, p. Th.1.D.4.

[29] P. Poggiolini, G. Bosco, A. Carena, V. Curri, Y. Jiang, and F. Forghieri, "The GN-model of fiber non-linear propagation and its applications," *J. Lightw. Technol.*, vol. 32, no. 4, pp. 694–721, Feb. 2014.

[30] F. Vacondio, O. Rival, C. Simonneau, E. Grellier, A. Bononi, L. Lorcy, J.-C. Antona, and S. Bigo, "On nonlinear distortions of highly dispersive optical coherent systems," *Opt. Express*, vol. 20, no. 2, pp. 1022–1032, Jan. 2012.

Pontus Johannisson received his Ph.D. degree from Chalmers University of Technology, Gothenburg, Sweden, in 2006. His thesis was focused on nonlinear intrachannel signal impairments in optical fiber communications systems.

In 2006, he joined the research institute IMEGO in Gothenburg, Sweden, where he worked with digital signal processing for inertial navigation with MEMS-based accelerometers and gyroscopes. In 2009, he joined the Photonics Laboratory, Chalmers University of Technology, where he currently holds a position as Assistant Professor. A significant part of his time is spent working on cross-disciplinary topics within the Fiber-Optic Communications Research Center (FORCE) at Chalmers. His research interests include, e.g., nonlinear effects in optical fibers and digital signal processing in coherent optical receivers.

Erik Agrell (M'99–SM'02) received the Ph.D. degree in information theory in 1997 from Chalmers University of Technology, Sweden.

From 1997 to 1999, he was a Postdoctoral Researcher with the University of California, San Diego and the University of Illinois at Urbana-Champaign. In 1999, he joined the faculty of Chalmers University of Technology, first as an Associate Professor and since 2009 as a Professor in Communication Systems. In 2010, he cofounded the Fiber-Optic Communications Research Center (FORCE) at Chalmers, where he leads the signals and systems research area. His research interests belong to the fields of information theory, coding theory, and digital communications, and his favorite applications are found in optical communications.

Prof. Agrell served as Publications Editor for the IEEE Transactions on Information Theory from 1999 to 2002 and is an Associate Editor for the IEEE Transactions on Communications since 2012. He is a recipient of the 1990 John Ericsson Medal, the 2009 ITW Best Poster Award, the 2011 GlobeCom Best Paper Award, the 2013 CTW Best Poster Award, and the 2013 Chalmers Supervisor of the Year Award.